Article Information

Journal Title: ASME 2018 International Technical Conference and Exhibition on Packaging and Integration of Electronic and Photonic Microsystems : August 27-30, 2018,

Volume: **Issue:**
Month/Year: 2018 **Pages:** -

Article Author: Boteler, L M

Article Title: Comparison of Thermal and Stress Analysis Results for a High Voltage Module Using FEA and a Quick Parametric Analysis Tool

Loan Information

Loan Title: ASME 2018 International Technical Conference and Exhibition on Packaging and Integration of Electronic and Photonic Microsystems : August 27-30, 2018, Comparison of Thermal and Stress Analysis Results for a High Voltage Module Using FEA and a Quick Parame

Loan Author: Boteler, L M

Publisher: New York, N.Y. : American Society of Mechanical En
Place:
Date: 2018
Imprint:

Borrowing Library Information

Library Name: N.I.H. Library- Interlibrary Loan Unit (HNI)

Bldg.10, Rm.B1L-306
10 Center Drive, MSC 1150
Bethesda, Maryland 20892-1150

Patron:
Fax: (301) 402-1200
Ariel Address: 137.187.166.147
Borrowing Dept. EMail: ill@nihrrlib.ncrr.nih.gov

Ship Article Via: Article Exchange

Borrowing Notes: Borrowing Notes: ***Please do not Ariel any articles to us since our Ariel System is down at this time. Thank you!!!

Proceedings of the ASME 2018 International Technical Conference and Exhibition on Packaging and Integration of Electronic and Photonic Microsystems
InterPACK2018
August 27-30, 2018, San Francisco, CA, USA

IPACK2018-8394

Comparison of Thermal and Stress Analysis Results for a High Voltage Module Using FEA and a Quick Parametric Analysis Tool

L. M. Boteler
U.S. Army Research Laboratory
Adelphi, MD, USA

S. M. Miner
U.S. Naval Academy
Annapolis, MD, USA

ABSTRACT

A low order fast running parametric analysis tool, ParaPower, was used to arrive at the design for a novel high voltage module. The low order model used a 3D nodal network to calculate device temperatures and thermal stresses. The model assumed heat flux generated near the top surface of each device which is then conducted through the packaging structure and removed by convection. The temperature distribution is used to calculate thermal stresses throughout the package. This co-design modeling tool, developed for rectilinear geometries, allowed a rapid evaluation of the package temperatures and CTE induced stresses throughout the design space. However, once the final design configuration was determined a detailed finite element analysis was performed to validate the design. This paper compares the results obtained using ParaPower to the FEA, demonstrating the usefulness of the parametric analysis tool. Results for both temperature and CTE induced stress are compared. Two different stress models are evaluated. One based on the more traditional planar module design, which assumes a substantial substrate or heat spreader on which the module is assembled. The other model is less restrictive, eliminating the requirement for a substrate. The FEA modeling was performed using SolidWorks beginning with a thermal analysis followed by a stress analysis based on the temperature solution. Both the values and the trends of the temperatures and stresses were evaluated. The temperature results agreed to within 3.2ºC. The trends and sign of the stresses were correctly predicted, but the magnitudes were not. One of the significant advantages of ParaPower is the speed of the computation. The run time for the parametric analysis was roughly two orders of magnitude faster than the FEA. This made it possible to build the model and complete the parametric analysis of roughly 500 runs in less than a day.

INTRODUCTION

In previous work [1], the authors demonstrated the use of a co-design approach in the ParaPower parametric analysis tool. The parametric analysis combined the thermal and CTE stress analyses providing an evaluation that addressed both aspects simultaneously. The analysis was applied to a typical planar type power module geometry, shown in figure 1.

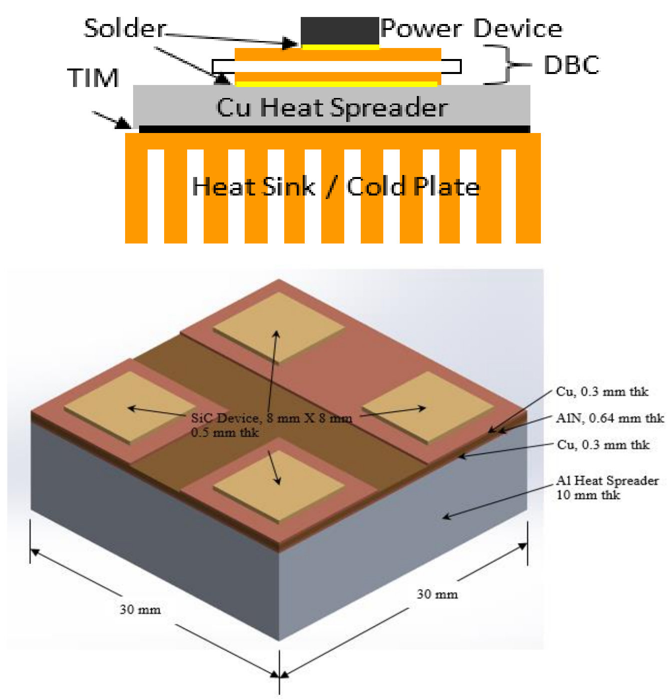

Figure 1: Schematic of a Standard Power Module

Validation against standard FEA results showed that the temperatures were predicted to within 3.5°C and the stresses to within 30%. The time required to obtain the results using the ParaPower tool was roughly two orders of magnitude faster than the FEA.

In the present study the parametric analysis tool is used to evaluate the design space for a novel stacked geometry. The new approach stacks power devices between copper sheets with an integrated cooling solution. By stacking devices, the module is no longer constrained by the limitations of planar packaging. However it is limited by the ability to remove heat. The heat removal challenge is solved by using double sided cooling, placing the heat sink in direct contact with both sides of each die. The structure becomes a five layer stack (copper, die, copper, die, copper) with the copper layers being multi-functional components (MFCs), simultaneously providing thermal, structural, and electrical contacts between the power die. Validation of the results is made through a comparison to thermal and stress FEA results.

NOMENCLATURE

E – Young's modulus
F_x – x direction force
F_y – y direction force
L_F – Final length
L_o – Initial length
L_T – Unrestrained expansion/contraction length
T – Temperature
c – Uniform component of strain
r – Radius of curvature
t_b – Bending axis location
z – Vertical location in the substrate/film stack
α - Coefficient of thermal expansion
ε - Strain
ν - Poisson's ratio
σ - Stress

GEOMETRY

Figure 2 shows the core of the stacked geometry. The copper sections pass through the AlN fins and are thermally connected to them and thermally connected to the SiC die. The copper pieces provide the thermal connections, electrical connections and the supporting structure for the die. The diodes are 10mm x 10mm. The active area is 5mm x 5mm on one side in the center with a heat generation rate of 1.6 W/mm^2. The AlN fins are 18mm x 18mm and 3mm thick with a 5mm x 5mm cut out in the center to accommodate the copper connectors. This core is placed inside a copper casing filled with an epoxy encapsulant that provides voltage stand-off. The casing is finned (not shown) to provide enhanced surface area for convection. The AlN fins are thermally connected to the case and the ends are capped with plastic end caps. Figure 3 shows the assembled geometry. The overall package size is 33mm x 33mm x 22mm.

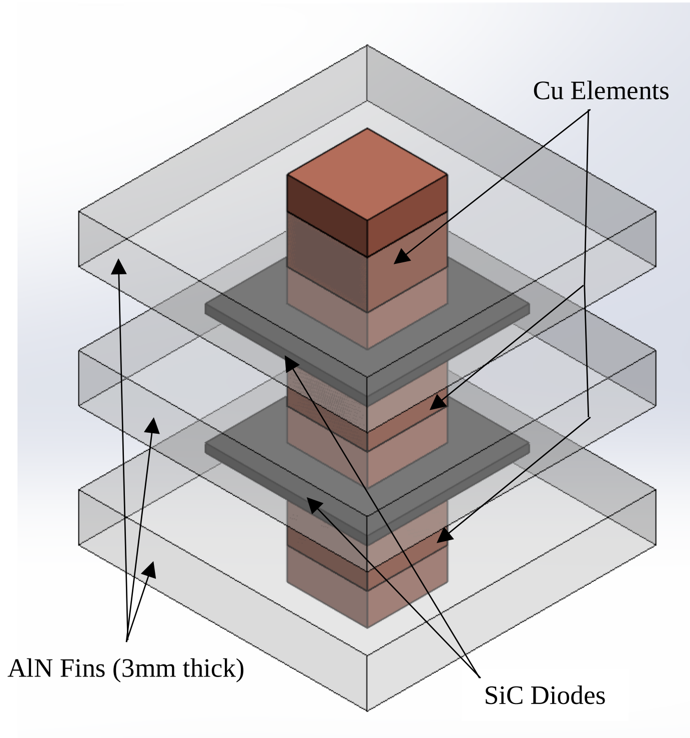

Figure 2: Core Geometry

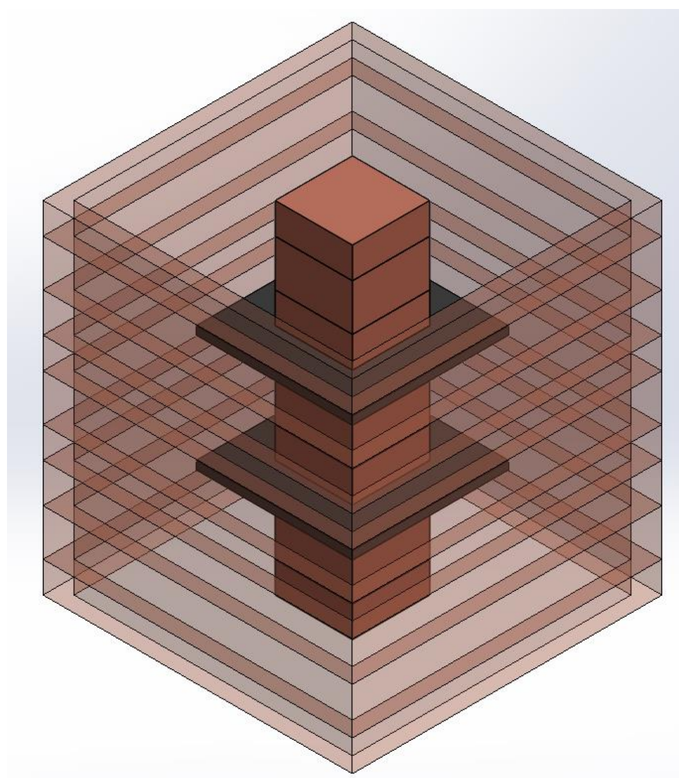

Figure 3: Overall Assembly

THERMAL STRESS MODEL

In the previous work the thermal stress analysis outlined by Hsueh [2] was the approach used. That analysis treats the system as a substrate layer on which the other film layers are stacked. The equations for the stress in the substrate and the individual film layers are:

$$\begin{aligned} \sigma_S &= E_S\left(\varepsilon - \sigma_S \Delta T\right) \quad \text{stress in the substrate,} \\ \sigma_i &= E_i\left(\varepsilon - \sigma_i \Delta T\right) \quad \text{stress in individual film layers.} \end{aligned} \tag{1}$$

In both equations the value for E is the biaxial modulus given by $E/\left(1-\nu\right)$. This accounts for two dimensional planar stress, as opposed to a single dimension uniaxial stress. At each layer in the assembly, substrate and film(s), the stress distribution is assumed to be planar. The value of ε is given by $\varepsilon = c + \frac{z-t_b}{r}$, where the first term on the right represents the contribution to stress from the uniform strain component and the second term is the contribution from the bending strain. In this paper the exact formulation proposed by Hsueh is used. This formulation is appropriate for the planar geometry of Figure 1, but not as applicable to the stacked geometry of Figures 2 and 3.

As a result an alternate stress model was developed that didn't impose the substrate requirement of Hsueh's model. In this model the elements in each layer are first allowed to expand or contract (L_{Ti}) based on the difference in temperature between the processing temperature and the operating temperature. Then the strain for that element is based on the difference between that element's length and final length of all the elements (L_F) in that stack of elements. The final length is based on the equilibrium of the forces in all the elements in that stack of elements. The outline of the formulation follows.

$$\begin{aligned} & L_{Ti} = L_o(\alpha_i \Delta T_i + 1) \\ & \varepsilon_i = \left(L_F - L_{Ti}\right)/L_{Ti} \\ & \sigma_i = \varepsilon_i E_i \\ & F_{ix} = \sigma_i dydz \qquad F_{iy} = \sigma_i dxdz \\ & \sum F_{ix} = 0 \qquad \sum F_{iy} = 0 \\ & L_{Fx} = \frac{\left(L_o \sum E_i dydz\right)}{\sum \frac{(E_i dydz)}{(\alpha_i \Delta T_i + 1)}} \\ & L_{Fy} = \frac{\left(L_o \sum E_i dxdz\right)}{\sum \frac{(E_i dxdz)}{(\alpha_i \Delta T_i + 1)}} \end{aligned} \tag{2}$$

It should be noted that both stress formulations are based only on the temperature difference between the zero stress processing temperature and the operating temperature of each particular element. This accounts for inter-layer differences in stress. It does not account for the intra-layer, or edge effects that result from the interface of differing geometries, materials or both. Including these effects would significantly increase the complexity of the model and the time required to generate a solution.

RESULTS

Parametric Study

The primary benefit of the technique presented in this paper is the ability to complete parametric studies in short periods of time. This allows evaluation of the design space in order to pick the best design, based on thermal and mechanical considerations. A total of roughly 500 runs were performed and they were all completed in 24 seconds. Model size for these runs was 14 layers with an 11 x 11 mesh of elements for each layer. This made to total model size 1694 elements. Parameters evaluated included, exterior convection coefficient, the number of fins, fin thickness, fin conductivity and the stress model. Table 1 lists the values of the various parameters considered.

Table1: design Space Parameters

Parameter	Value						
h (W/m^2 C)	1000	2500	5000	7500	10000	12500	15000
No. of Fins	1	2	3	4	6	9	
Thk (mm)	1	2	3	4	5		
k (W/m C)	25	100	160				
Stress	Hsueh	Alt					

Figures 3, 4 and 5 illustrate the types of results that are generated by the parametric analysis.

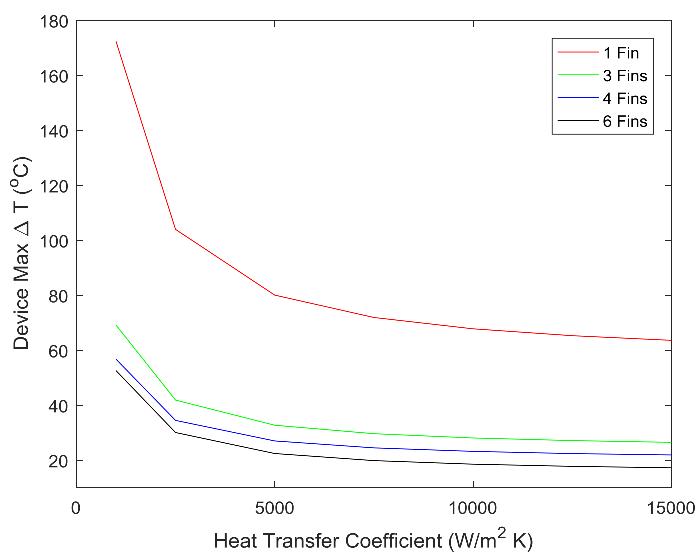

Figure 3: Effect of Number of Fins on Temperature (3 mm thick fins)

temperature penalty. As a result of the parametric study, the geometry shown in figures 2 and 3 was selected. It has 3, 3mm thick fins and uses a convection coefficient of 5000 W/m^2 K.

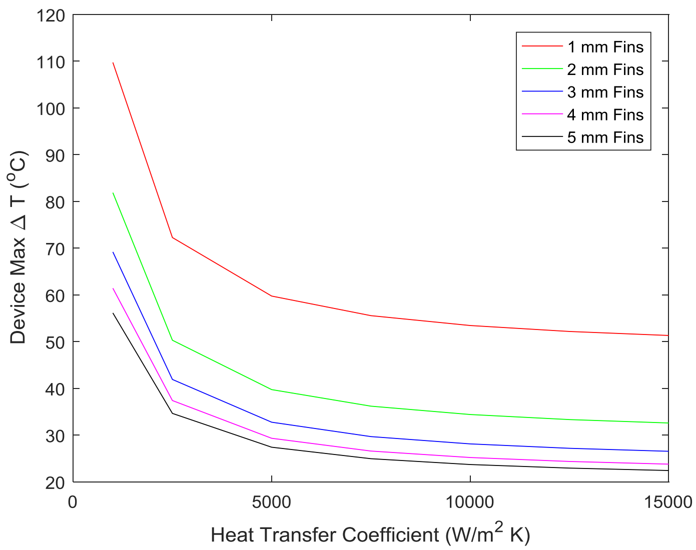

Figure 4: Effect of Fin Thickness on Temperature (3 fins)

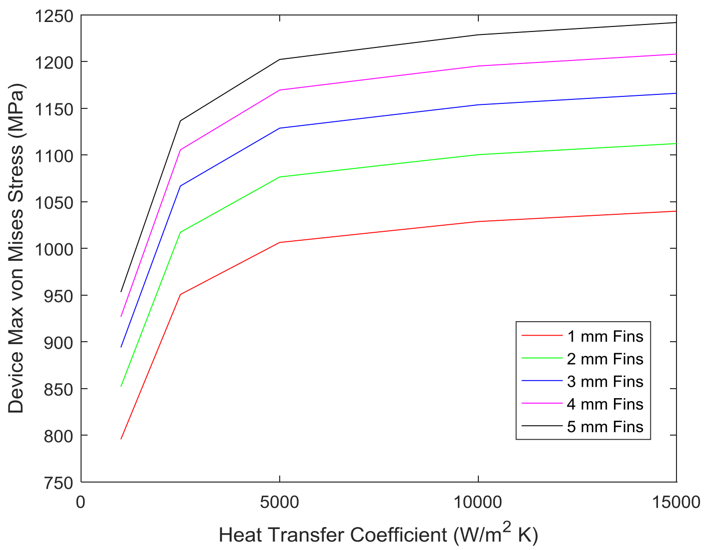

Figure 5: Effect of Fin Thickness on Stress (3 Fins)

Figure 3 shows the effect of the number of fins on the device maximum temperature, indicating that more than 3 fins and a convection coefficient greater than 5000 W/m^2 K does not provide a large decrease in device temperature. Figure 4 illustrates the effect of fin thickness on device maximum temperature, indicating that fin thicknesses greater than 3mm do not significantly reduce the device maximum temperature. Figure 5 shows that the device stress is significantly lower at convection coefficients less than 5000 W/m^2 K and lower number of fins, but this benefit would come with a significant temperature penalty.

Comparison to FEA

Verification of the temperature and stress results from the parametric study for the final design was performed using SolidWorks finite element analysis for the temperatures and stresses for the same geometry. Figures 6 and 7 show the mesh for the core and overall assembly, respectively. The mesh contained a total of 73578 elements and required 9 seconds to generate. The thermal analysis required 13 seconds to execute

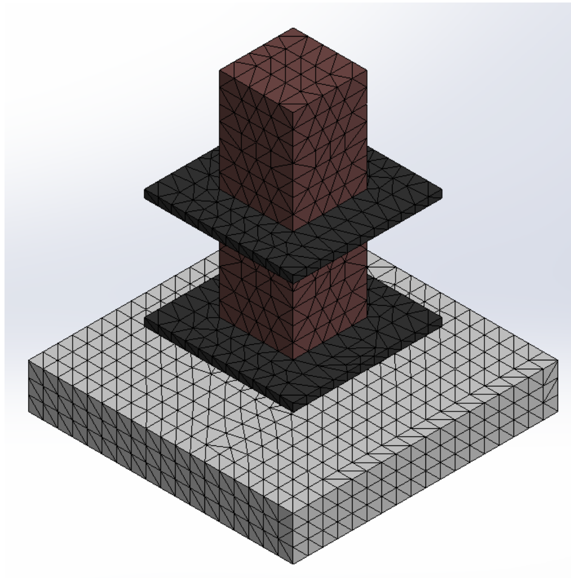

Figure 6: Core Mesh, Top and Center Fins Removed to show Detail

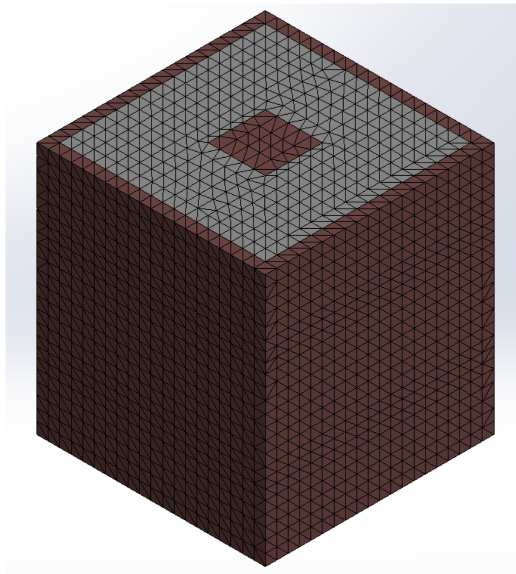

Figure 7: Overall Assembly Mesh

and the subsequent stress analysis required 15 seconds. This was for a single run.

Figures 8 and 9 show the temperature results for the upper and lower devices. The same temperature scale is used in both figures to make comparison between the devices easier.

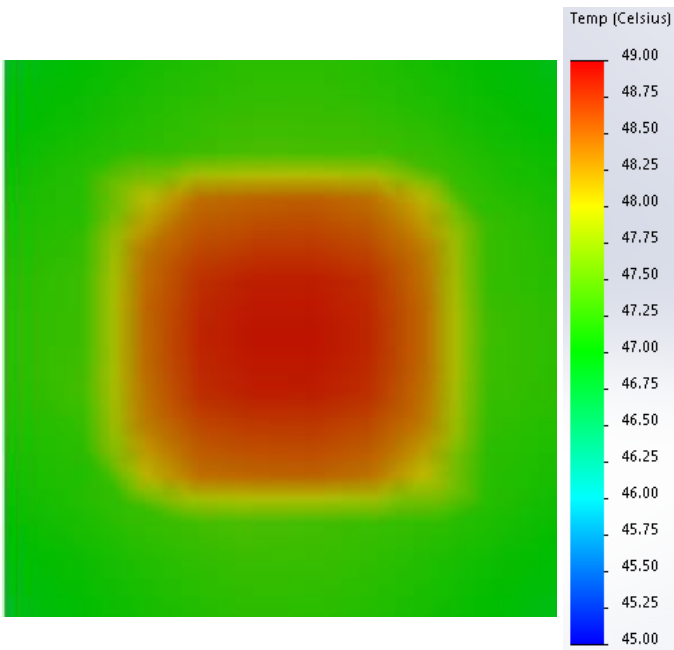

50.2	50.4	50.5	50.4	50.2
50.4	51.9	52.0	51.9	50.4
50.5	52.0	52.1	52.0	50.5
50.4	51.9	52.0	51.9	50.4
50.2	50.4	50.5	50.4	50.2

Figure 8: Upper Device Temperature (ºC)

For both devices the maximum temperatures agree to within 3.5ºC and the temperature distributions across the device also agree to within 3.5ºC. Also, the temperature difference between the two devices is also properly reflected in the results. Figures 10, 11 and 12 show the temperature results for the upper, center and lower fins, respectively. Again, the same temperature scale is used in all three figures to make comparison easier. The FEA results are on the top and bottom surfaces of the fin, whereas the parametric study results are at the center. As with the device comparison, the parametric study results properly capture the temperature distributions and differences between the three fins. Again, the temperatures agree to within 3.5ºC. As a final

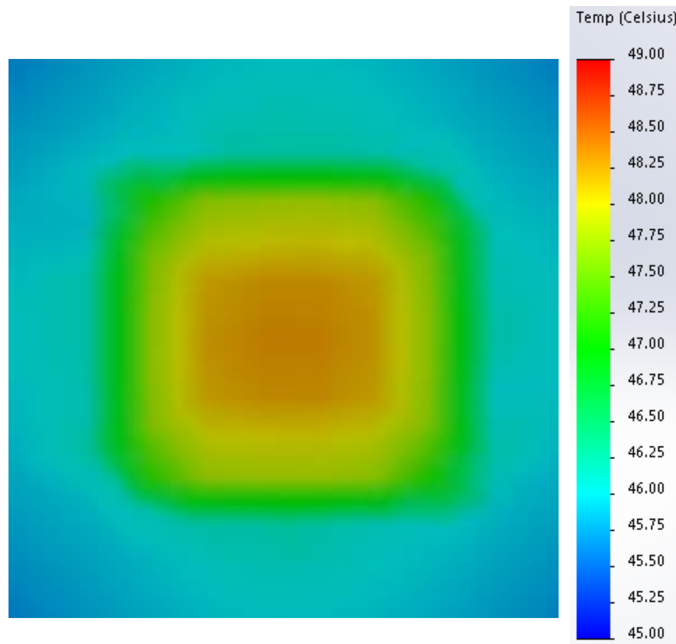

48.9	49.1	49.1	49.1	48.9
49.1	51.3	51.4	51.3	49.1
49.1	51.4	51.5	51.4	49.1
49.1	51.3	51.4	51.3	49.1
48.9	49.1	49.1	49.1	48.9

Figure 9: Lower Device Temperature (ºC)

comparison of temperature results, figure 13 shows the temperature distribution on the outside surface of the overall assembly. The peak temperatures and the distribution are properly captured.

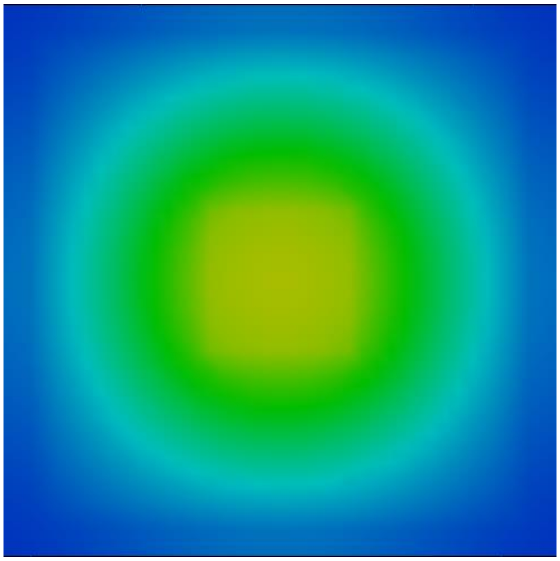

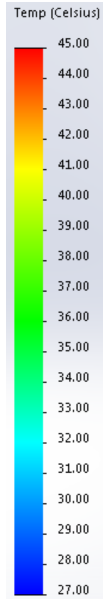

28.7	28.9	29.4	30.0	30.4	30.5	30.4	30.0	29.4	28.9	28.7
28.9	29.4	30.2	31.1	31.6	31.8	31.6	31.1	30.2	29.4	28.9
29.4	30.2	31.5	33.0	34.1	34.4	34.1	33.0	31.5	30.2	29.4
30.0	31.1	33.0	35.4	37.7	38.2	37.7	35.4	33.0	31.1	30.0
30.4	31.6	34.1	37.7	42.0	42.6	42.0	37.7	34.1	31.6	30.4
30.5	31.8	34.4	38.2	42.6	43.1	42.6	38.2	34.4	31.8	30.5
30.4	31.6	34.1	37.7	42.0	42.6	42.0	37.7	34.1	31.6	30.4
30.0	31.1	33.0	35.4	37.7	38.2	37.7	35.4	33.0	31.1	30.0
29.4	30.2	31.5	33.0	34.1	34.4	34.1	33.0	31.5	30.2	29.4
28.9	29.4	30.2	31.1	31.6	31.8	31.6	31.1	30.2	29.4	28.9
28.7	28.9	29.4	30.0	30.4	30.5	30.4	30.0	29.4	28.9	28.7

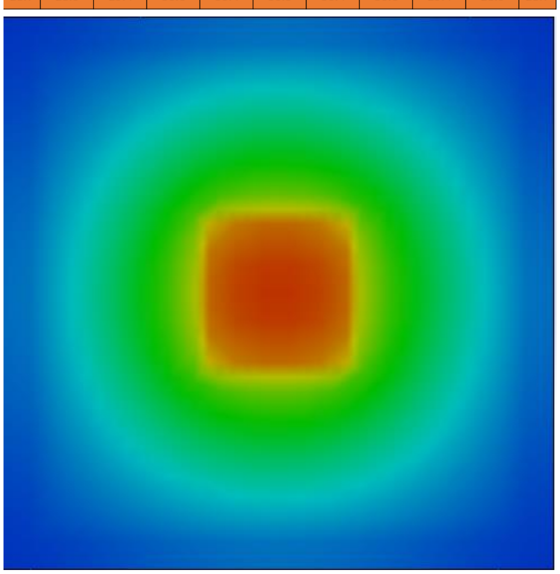

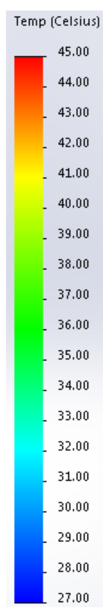

Figure 10: Upper Fin Temperature (^oC)

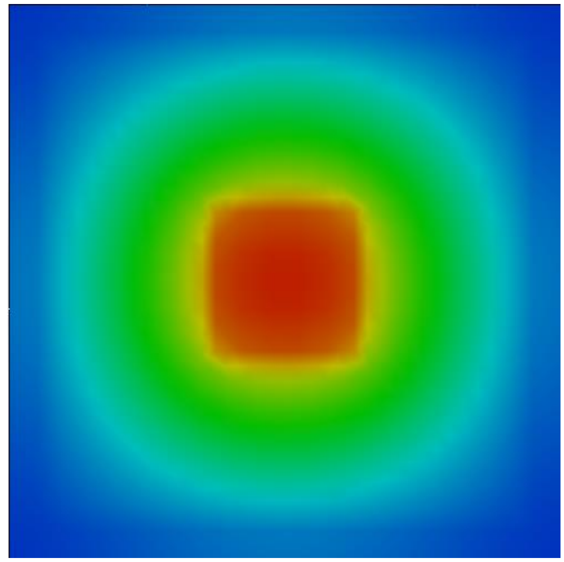

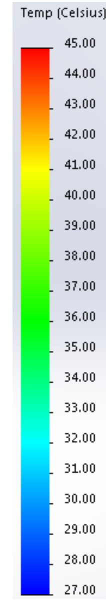

28.7	29.0	29.5	30.2	30.6	30.7	30.6	30.2	29.5	29.0	28.7
29.0	29.5	30.4	31.4	32.1	32.2	32.1	31.4	30.4	29.5	29.0
29.5	30.4	32.0	33.7	35.0	35.3	35.0	33.7	32.0	30.4	29.5
30.2	31.4	33.7	36.6	39.3	40.0	39.3	36.6	33.7	31.4	30.2
30.6	32.1	35.0	39.3	44.5	45.1	44.5	39.3	35.0	32.1	30.6
30.7	32.2	35.3	40.0	45.1	45.7	45.1	40.0	35.3	32.2	30.7
30.6	32.1	35.0	39.3	44.5	45.1	44.5	39.3	35.0	32.1	30.6
30.2	31.4	33.7	36.6	39.3	40.0	39.3	36.6	33.7	31.4	30.2
29.5	30.4	32.0	33.7	35.0	35.3	35.0	33.7	32.0	30.4	29.5
29.0	29.5	30.4	31.4	32.1	32.2	32.1	31.4	30.4	29.5	29.0
28.7	29.0	29.5	30.2	30.6	30.7	30.6	30.2	29.5	29.0	28.7

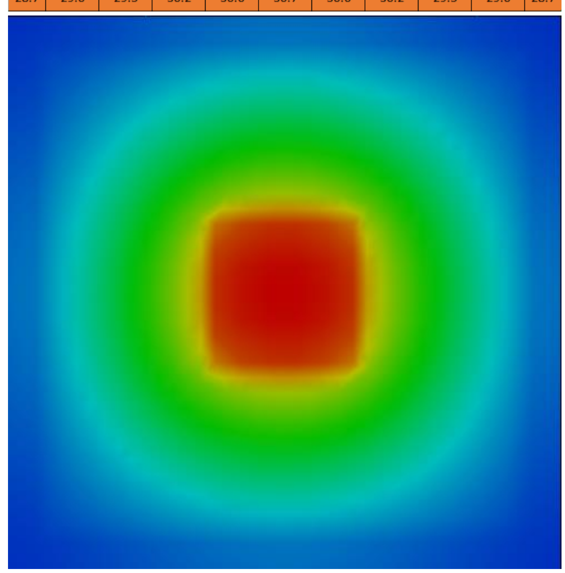

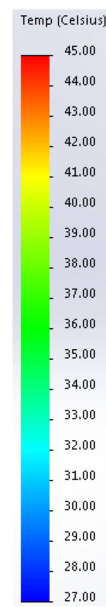

Figure 11: Center Fin Temperature (^oC)

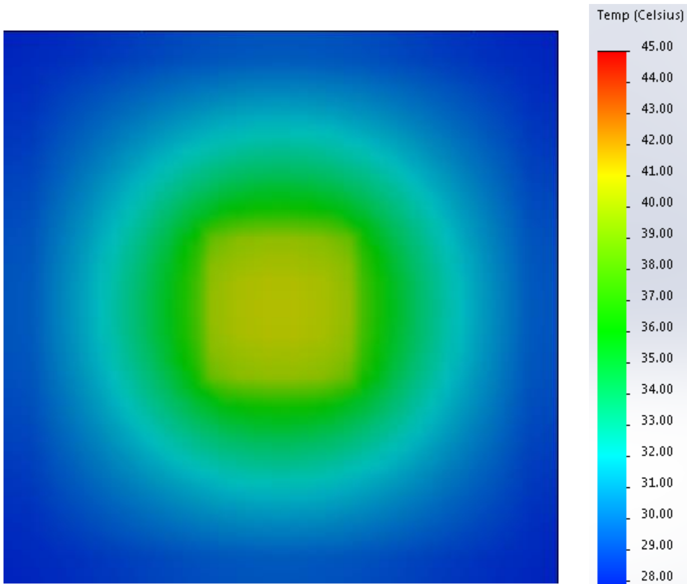

28.2	28.4	28.8	29.3	29.6	29.7	29.6	29.3	28.8	28.4	28.2
28.4	28.8	29.5	30.2	30.6	30.8	30.6	30.2	29.5	28.8	28.4
28.8	29.5	30.6	31.8	32.7	32.9	32.7	31.8	30.6	29.5	28.8
29.3	30.2	31.8	33.9	35.7	36.2	35.7	33.9	31.8	30.2	29.3
29.6	30.6	32.7	35.7	39.4	39.8	39.4	35.7	32.7	30.6	29.6
29.7	30.8	32.9	36.2	39.8	40.3	39.8	36.2	32.9	30.8	29.7
29.6	30.6	32.7	35.7	39.4	39.8	39.4	35.7	32.7	30.6	29.6
29.3	30.2	31.8	33.9	35.7	36.2	35.7	33.9	31.8	30.2	29.3
28.8	29.5	30.6	31.8	32.7	32.9	32.7	31.8	30.6	29.5	28.8
28.4	28.8	29.5	30.2	30.6	30.8	30.6	30.2	29.5	28.8	28.4
28.2	28.4	28.8	29.3	29.6	29.7	29.6	29.3	28.8	28.4	28.2

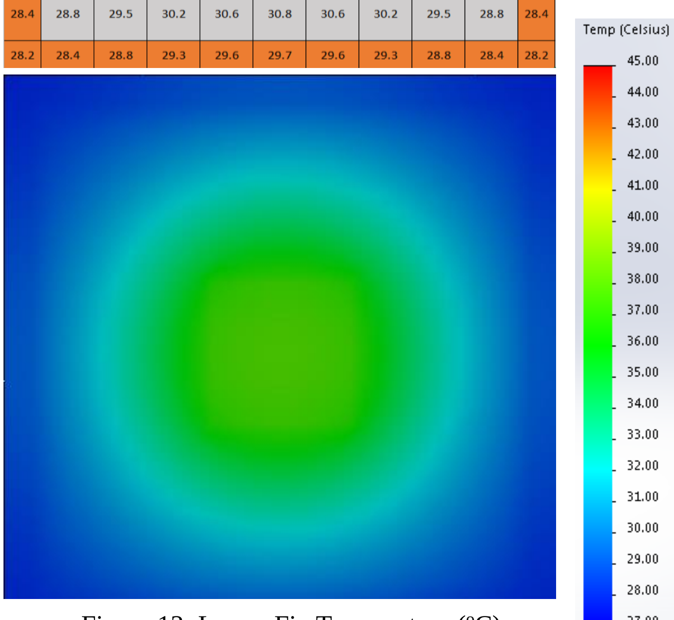

Figure 12: Lower Fin Temperature (°C)

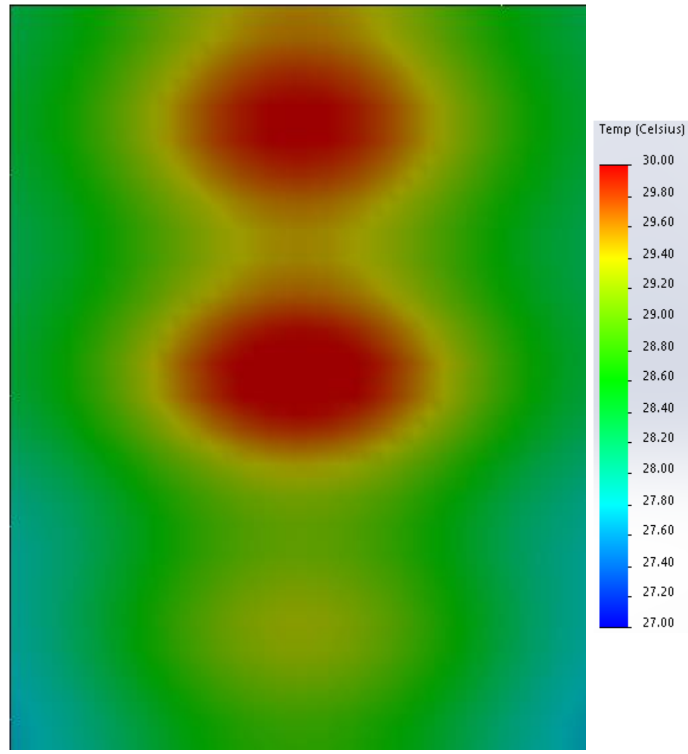

28.5	28.6	28.9	29.3	29.5	29.6	29.5	29.3	28.9	28.6	28.5
28.7	28.9	29.4	30.0	30.4	30.5	30.4	30.0	29.4	28.9	28.7
28.4	28.6	28.9	29.3	29.5	29.6	29.5	29.3	28.9	28.6	28.4
28.4	28.6	28.9	29.3	29.5	29.6	29.5	29.3	28.9	28.6	28.4
28.4	28.5	28.9	29.2	29.5	29.6	29.5	29.2	28.9	28.5	28.4
28.5	28.6	28.9	29.3	29.6	29.6	29.6	29.3	28.9	28.6	28.5
28.7	29.0	29.5	30.2	30.6	30.7	30.6	30.2	29.5	29.0	28.7
28.3	28.4	28.7	29.1	29.4	29.4	29.4	29.1	28.7	28.4	28.3
28.2	28.3	28.6	29.0	29.2	29.2	29.2	29.0	28.6	28.3	28.2
28.2	28.3	28.6	28.9	29.1	29.2	29.1	28.9	28.6	28.3	28.2
28.1	28.2	28.5	28.8	29.0	29.1	29.0	28.8	28.5	28.2	28.1
28.2	28.4	28.8	29.3	29.6	29.7	29.6	29.3	28.8	28.4	28.2
27.9	28.0	28.3	28.6	28.8	28.9	28.8	28.6	28.3	28.0	27.9

Figure 13: Side Wall Temperature (°C)

The other part of the verification involves comparing the stresses for the parametric and FEA results. These comparisons are shown for the upper device and the center fin in figures 14 and 15. For this comparison the principle stress is used.

-146.8	-141.5	-140.2	-141.5	-146.8
-141.5	-1452.1	-1449.4	-1452.1	-141.5
-140.2	-1449.4	-1446.8	-1449.4	-140.2
-141.5	-1452.1	-1449.4	-1452.1	-141.5
-146.8	-141.5	-140.2	-141.5	-146.8

Hsueh

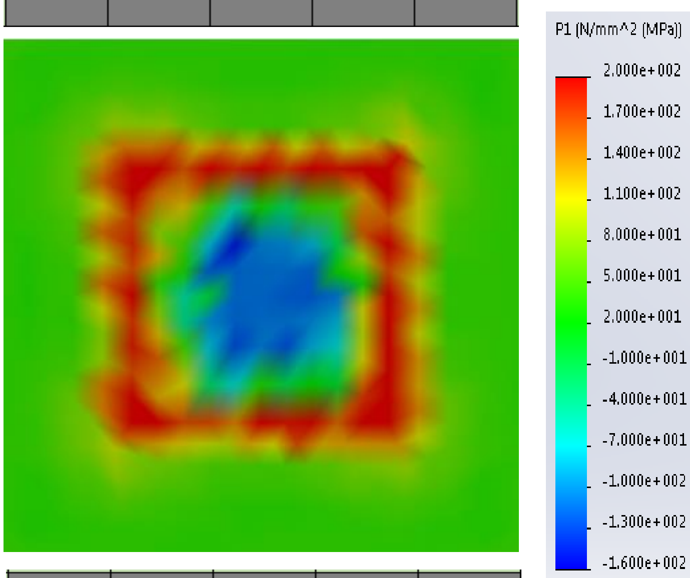

-117.2	-113.0	-112.0	-113.0	-117.2
-113.0	-1133.2	-1131.1	-1133.2	-113.0
-112.0	-1131.1	-1129.0	-1131.1	-112.0
-113.0	-1133.2	-1131.1	-1133.2	-113.0
-117.2	-113.0	-112.0	-113.0	-117.2

Alt

Figure 14 Upper Device Stress (MPa)

-1.5	-1.8	-2.5	-3.3	-3.8	-3.9	-3.8	-3.3	-2.5	-1.8	-1.5
-1.8	-54.6	-54.6	-54.6	-54.6	-54.6	-54.6	-54.6	-54.6	-54.6	-1.8
-2.5	-54.6	-54.5	-54.4	-54.5	-54.5	-54.5	-54.4	-54.5	-54.6	-2.5
-3.3	-54.6	-54.4	-32.8	-33.7	-33.9	-33.7	-32.8	-54.4	-54.6	-3.3
-3.8	-54.6	-54.5	-33.7	73.2	71.6	73.2	-33.7	-54.5	-54.6	-3.8
-3.9	-54.6	-54.5	-33.9	71.6	70.1	71.6	-33.9	-54.5	-54.6	-3.9
-3.8	-54.6	-54.5	-33.7	73.2	71.6	73.2	-33.7	-54.5	-54.6	-3.8
-3.3	-54.6	-54.4	-32.8	-33.7	-33.9	-33.7	-32.8	-54.4	-54.6	-3.3
-2.5	-54.6	-54.5	-54.4	-54.5	-54.5	-54.5	-54.4	-54.5	-54.6	-2.5
-1.8	-54.6	-54.6	-54.6	-54.6	-54.6	-54.6	-54.6	-54.6	-54.6	-1.8
-1.5	-1.8	-2.5	-3.3	-3.8	-3.9	-3.8	-3.3	-2.5	-1.8	-1.5

Hsueh

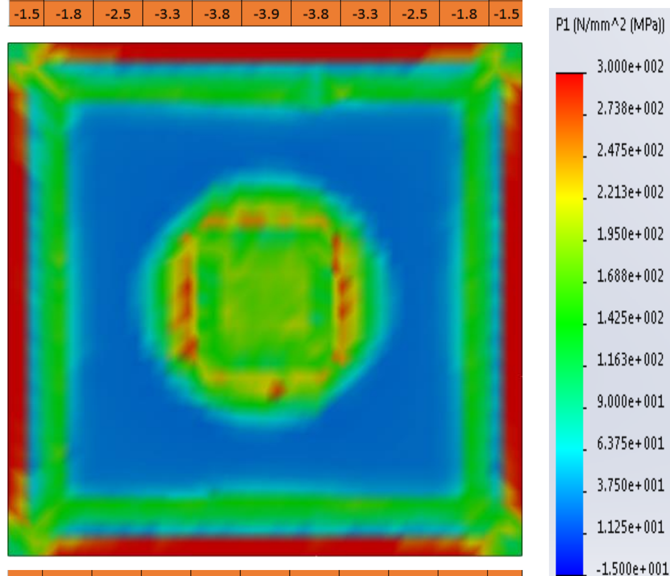

21.7	21.5	21.0	20.4	20.1	20.0	20.1	20.4	21.0	21.5	21.7
21.5	-33.4	-33.5	-33.5	-33.6	-33.6	-33.6	-33.5	-33.5	-33.4	21.5
21.0	-33.5	-33.5	-33.4	-33.5	-33.6	-33.5	-33.4	-33.5	-33.5	21.0
20.4	-33.5	-33.4	-16.8	-17.6	-17.8	-17.6	-16.8	-33.4	-33.5	20.4
20.1	-33.6	-33.5	-17.6	79.4	78.4	79.4	-17.6	-33.5	-33.6	20.1
20.0	-33.6	-33.6	-17.8	78.4	77.3	78.4	-17.8	-33.6	-33.6	20.0
20.1	-33.6	-33.5	-17.6	79.4	78.4	79.4	-17.6	-33.5	-33.6	20.1
20.4	-33.5	-33.4	-16.8	-17.6	-17.8	-17.6	-16.8	-33.4	-33.5	20.4
21.0	-33.5	-33.5	-33.4	-33.5	-33.6	-33.5	-33.4	-33.5	-33.5	21.0
21.5	-33.4	-33.5	-33.5	-33.6	-33.6	-33.6	-33.5	-33.5	-33.4	21.5
21.7	21.5	21.0	20.4	20.1	20.0	20.1	20.4	21.0	21.5	21.7

Alt

Figure 15 Center Fin Stress (MPa)

Both models used for the parametric results assume a planar state of stress that evaluates only the normal stress components. The FEA computes the full 3-D stress field, but the geometry as analyzed produces an essentially biaxial state of stress. As a result the principle stress is used for comparison. This will allow both the magnitude and the sign of the stresses to be compared. Only the upper device and the center fin comparisons are shown, as the stress levels and distributions are essentially the same for both devices and the three fins. Figure 14 shows that while the sign of the stress is correctly captured by the parametric analysis, the magnitude of the stress is grossly over predicted. The relationship of the order of magnitude of the stress between the center portion and the perimeter is correctly evaluated, roughly an order of magnitude lower in the perimeter. This makes sense as the center portion is in contact with the copper bar, while the perimeter is in contact with the epoxy encapsulant. The encapsulant has a much lower value of E, which would make it much less able to exert a compressive force on the SiC. Figure 15 shows the comparison for the fins. Here the agreement is much better both in terms of the magnitude and the sign of the stress. In both cases the alternate stress model does a better job, which is likely due to eliminating the substrate assumption that is present in the model by Hseuh. Given that the stress models used in the parametric analysis do not adequately predict the magnitude of the stress for SiC devices, it is of interest to see if the trends are at least correctly predicted. Figures 16 and 17 address this trend issue, by comparing center point temperatures and stresses for the upper device. In the case of the device stress the results are normalized to the stress at 1000 W/m^2 K, so that the shape of the trend lines can be compared.

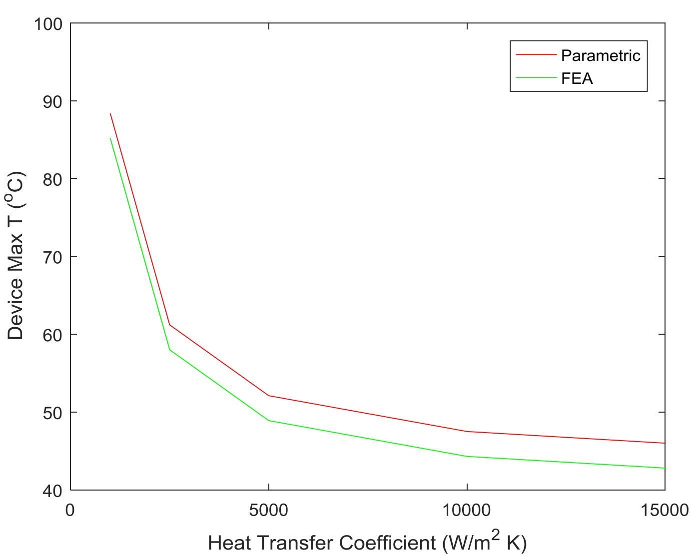

Figure 16: Temperature Trend Comparison

Figure 16 shows that both the temperature and the trend for the upper device center point temperature are accurately captured. The difference in temperature across the range of convection coefficients is 3.2ºC. Figure 17 shows that the trend in the upper device center point stress is accurately captured by the parametric model, even if the magnitude is not. So, as a design space evaluation tool the parametric model does provide an adequate representation of the trends.

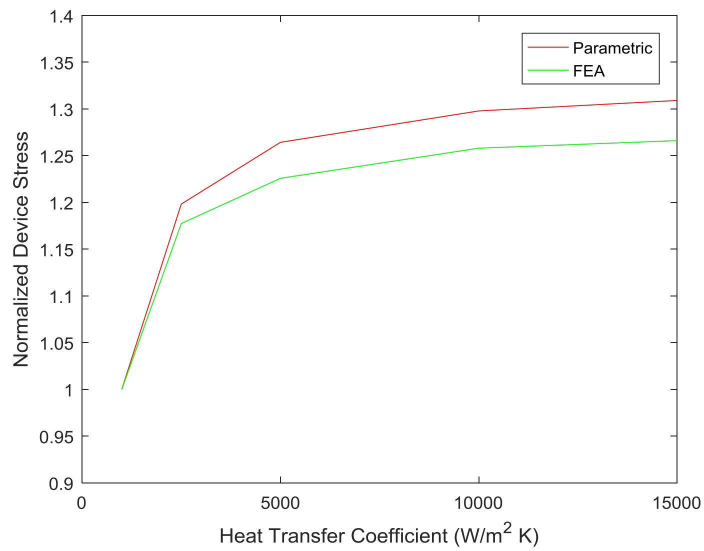

Figure 17: Stress Trend Comparison

As previously mentioned, neither stress model used in the parametric analysis includes the intra-layer, or edge effects that result from the interface of differing geometries, materials or both. Given the results above for the stresses it appears that some additional complexity in the stress model is needed to better capture the magnitudes. Including intra-layer effects should be considered.

CONCLUSIONS

ParaPower provides a low fidelity, high speed design tool for completing parametric studies in electronic packaging applications. It incorporates a co-design approach combining both the thermal and stress analysis in a single tool. Compared to standard FEA, ParaPower runs significantly faster, 24sec for 500 runs vice 37 sec for a single run. The parametric solution provides maximum device temperatures that are within 3.2ºC of the FEA. The parametric solution for the stresses shows the proper sign (tension/compression) and correctly predicts trends, but does not accurately predict the magnitude. This is a result of the simplified stress model used, which sacrifices detail for speed. Additional work in this area is needed to improve the stress predictions without an excessive time penalty. The value of ParaPower is the ability to effectively evaluate trade-offs during the design phase. The multi-domain parametric analysis enables packaging solutions that might not be realized through the traditional design cycle.

ACKNOWLEDGMENTS

The authors would like to thank colleagues at the U.S. Army Research Laboratory who have helped support this effort including Bruce Geil and Morris Berman.

REFERENCES

1. Boteler, L. M., Miner, S. M., “Power Packaging Thermal and Stress Model for Quick Parametric Analyses,” Proceedings of the ASME 2017 International Technical Conference and Exhibition on Packaging and Integration of Electronic and Photonic Microsystems, IPACK2017-74130, August 2017.
2. Hsueh, C. H., “Thermal Stresses in Elastic Multilayer Systems,” Thin Solid Films, Vol. 418, Elsevier